

Global spectral representations of black hole spacetimes in the complex plane

Maurice H.P.M. van Putten

MIT-LIGO, 175 Albany Street, NW17-161, Cambridge, MA 02139

Binary black hole coalescence produces a finite burst of gravitational radiation which propagates towards quiescent infinity. These spacetimes are analytic about infinity and contain a dimensionless coupling constant M/s , where M denotes the total mass-energy and s an imaginary distance. This introduces globally convergent Fourier series on a complex radial coordinate, allowing spectral representation of black hole spacetimes in all three dimensions. We illustrate this representation theory on a Fourier-Legendre expansion of Boyer-Lindquist initial data and a scalar wave equation with signal recovery by Cauchy's integral formula.

PACS numbers:

I. INTRODUCTION

Rapid progress in sensitivity in the broadband gravitational-wave observatories is creating new opportunities for searches for the bursts of gravitational-wave emissions produced by coalescing black holes. Detection strategies will benefit greatly from a priori understanding of their gravitational-wave emissions, which includes matched filtering techniques against a catalogue of signals precomputed by numerical relativity. This poses an interesting challenge of designing highly efficient and stable computational algorithms.

Numerical relativity is particularly challenging in calculating bursts and preceding chirps over many wave-periods in the presence of singularities associated with black hole spacetimes. Spectral methods provide an attractive approach. They are optimal in efficiency and accuracy, both in amplitude and phase, provided that the metric is smooth everywhere. Here, we focus on bursts of radiation produced by black hole coalescence which propagate towards quiescent infinity. By causality, these spacetimes preserve quiescence at infinity for all finite time.

The asymptotic structure of black hole spacetimes which are asymptotically flat and quiescent at infinity shares the same asymptotic properties as the Green's function of Minkowski spacetime. Consequently, these spacetimes carry a dimensionless coupling constant M/s , where M denotes the total mass-energy of the space. The Green's function of the Laplacean,

$$G(y^i, p^i) = \frac{1}{D(y^i, p^i)}, \quad (1)$$

is a function of the distance D between an observer at y^i and a source at p^i . We can expand G in Legendre polynomials P_l using a spherical coordinate system (r, θ, ϕ) ,

$$G = \frac{1}{\sqrt{r^2 + p^2 - 2pr \cos \theta}} = p^{-1} \sum \left(\frac{p}{r}\right)^{2l+1} P_{2l}(\cos \theta), \quad (2)$$

which shows that G is analytic in each coordinate away from the singularity at $y^i = p^i$ with domain of convergence $r > p$. We introduce complex distances through a

complex radial coordinate

$$z = x + is \quad (s > p). \quad (3)$$

The analytic continuation

$$G = p^{-1} \sum \left(\frac{p}{z}\right)^{2l+1} P_{2l}(\cos \theta) \quad (4)$$

is globally convergent on $-\infty < x < \infty$ outside $|z| = p$. (This corresponding branch cut for the square root is $(-\infty, 0]$.) To be precise: for each θ (4) defines a Taylor series in $1/z$ and, for each z , it defines a convergent expansion in Legendre functions. Thus, p/s is a running coupling constant and it must be less than one for convergence. We shall refer to M/s as the fixed coupling constant, noting that p/s is decreasing in binary coalescences.

Analyticity of the metric in $\text{Im}(z) \geq s$ defines an optimal distribution of points on $z = x + is$ for numerical implementation by the conformal transformation

$$w = \frac{M}{z} \quad (5)$$

Here, w describes a circle of radius $(2s)^{-1}$ about $w_0 = (2is)^{-1}$, whose interior corresponds to $\text{Im}(z) \geq s$. There exists a Taylor series in w about w_0 which is convergent up to including the boundary $C : w = (2is)^{-1} (e^{i\phi} + 1)$. The corresponding Fourier series in ϕ can be efficiently computed using the fast Fourier transform on a uniform distribution of points $\phi_k = 2^{-m+1} \pi k$ ($k = 1, 2, \dots, 2^m$) on C . Their images on $z = x + is$ produce the non-uniform distribution

$$z_k = Ms [\tan(\phi_k/2) + i], \quad (6)$$

whose large-scale cut-off is set by the proximity of the $\{\phi_k\}$ to $\pm\pi$.

We apply these observations to Boyer-Lindquist initial data for two black holes [5, 6], described by the potential

$$\Phi = 1 + \frac{M_1}{\sqrt{z^2 + p^2 - 2pz \cos \theta}} + \frac{M_2}{\sqrt{z^2 + q^2 - 2qz \cos \theta}} \quad (7)$$

for a pair of black holes with masses $M_{1,2}$ at positions p and q along the polar axis of a spherical coordinate

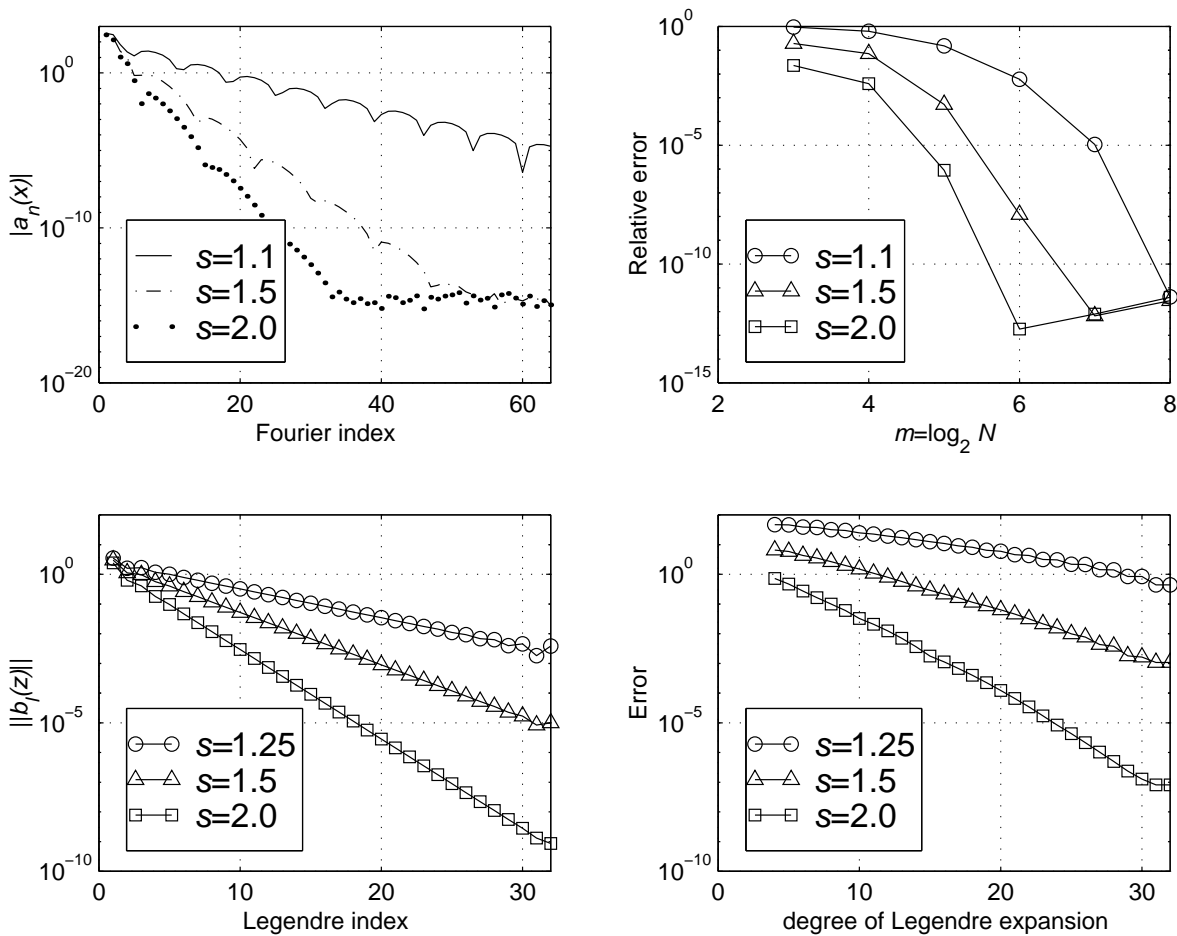


FIG. 1: The Boyer-Lindquist scalar field $\Phi(z, \theta)$ possesses a Fourier-Legendre expansion in $w = 1/z, z = x + is$, (top two windows) and $\cos \theta$ (bottom two windows), here shown for a symmetric configuration consisting of two black holes of mass $M_{1,2} = 1$ positioned at the north and south pole $p = \pm 1$ of a spherical coordinate system (r, θ, ϕ) . The Fourier coefficients show exponential decay by analyticity in $\text{Im}(z) \geq s > s^*(\theta) = p \sin \theta$ shown with $\cos \theta = 0.25$ and $s^* = 0.9682$. This gives rise to spectral accuracy in the first and second coordinate derivatives (top right). The norm of the Legendre coefficients shows exponential decay when s is larger than p (left). This gives rise to spectral accuracy in the first and second derivatives with respect to θ (bottom right).

system (r, θ, ϕ) . It will be appreciated that the singularities $z = pe^{\pm i\theta}$ are essential in making Φ non-trivial: the alternative of an entire function which is analytic at infinity would be constant by Liouville's theorem. For complex $z = x + is$ with s larger than both p and q , $\Phi(z, \theta)$ is finite and pointwise analytic everywhere on $-\infty + is < z < \infty + is$. Following (4) and (6), we capture analyticity by the Fourier-Legendre transform on the image $w = 1/z$. This gives rise to an efficient and accurate functional representation in (z, θ) with spectral accuracy in derivatives by spectral differentiation. Fig. 1 shows the computational results on the alternative representations

$$\Phi(z, \theta) = \sum_{n=1}^N a_n(\cos \theta) w^n = \sum_{l=0}^L b_l(z) P_l(\cos \theta), \quad (8)$$

where the series are finite in our numerical implementa-

tions.

The application to black holes spacetimes in the complex plane can be considered in the line-element

$$ds^2 = -N^2 dt^2 + h_{ij} dx^i dx^j, \quad N(z) = \frac{1 - M/2z}{1 + M/2z}, \quad (9)$$

for a three-metric h_{ij} . Working in the complex plane, we are at liberty to choose a lapse function N and vanishing shift functions in accord with the asymptotic Schwarzschild structure of spacetime at large distances. This applies without loss of generality to any binary black hole spacetime with total mass-energy M as measured at infinity, defined by the residue

$$M = \text{RE} \left\{ \frac{i}{\pi} \int_{-\infty + is}^{\infty + is} (h_{zz}^{1/4} - 1) dz \right\}. \quad (10)$$

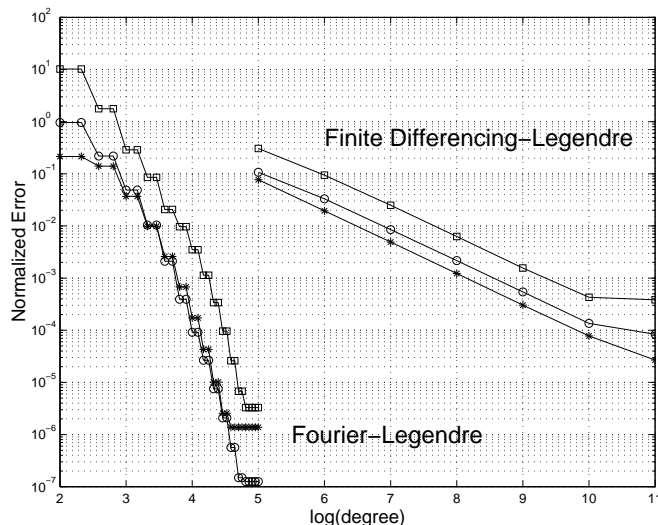


FIG. 2: Normalized errors in the first (*circles*) and second (*squares*) derivatives of the metric and the Ricci scalar tensor (*stars*) based on a Fourier-Legendre representation of Boyer-Lindquist initial data of Fig. 1 with $M/s = 1/2$. The Fourier-Legendre results are computed with $N = 32$ Fourier coefficients on $w = 1/z$ varying degrees $L = 4, \dots, 32$ of Legendre polynomials. The results are compared with a mixed finite differencing-Legendre method with varying degree $N = 2^m$, $m = 5, \dots, 11$ of the number of in the z -coordinate and fixed expansion in $L = 16$ Legendre polynomials. This comparison highlights the accuracy and efficiency of the Fourier-spectral method, even at low resolutions. The results are practically unchanged for other configurations of Boyer-Lindquist data, and the errors decrease for larger s .

For binary black hole coalescence, M is the sum $M_1 + M_2$ of the masses of the two black hole, plus the energy in gravitational radiation and minus the binding energy in the system. Thus, M is a constant. In contrast, M is a non-increasing function of time on any finite computational domain with outgoing radiation boundary conditions. For large z , the line-element (9) satisfies

$$ds^2 = -N^2 dt^2 + \left(1 + \frac{M}{2z}\right) (dz^2 + d\Sigma^2) + \dots \quad (11)$$

up to order $(M/z)^2$, where $d\Sigma^2 = z^2 d\theta^2 + z^2 \sin^2 \theta d\phi^2$ denotes the line-element of the coordinate sphere of radius z . Accordingly, the three-metric h_{ij} is decomposed into diagonal and off-diagonal elements given by the matrix factorization

$$h_{ij} = \gamma \begin{pmatrix} A_1^4 & B_1 & B_2 \\ B_1 & A_2^4 & B_3 \\ B_2 & B_3 & A_3^4 \end{pmatrix} \gamma, \quad (12)$$

where γ is the diagonal matrix

$$\gamma_{11} = 1, \gamma_{22} = z, \gamma_{33} = z \sin \theta. \quad (13)$$

In accord with the spectral representation of (4) and the potential (7), the coefficients (A_i, B_i) are expanded in spherical harmonics on $z = x + is$,

$$A_i = M \sum_{|m| \leq l} a_i^{ml}(t) w^{l+1} Y_{ml}(\theta, \phi), \quad (14)$$

$$B_i = M \sum_{|m| \leq l} b_i^{ml}(t) w^{l+1} Y_{ml}(\theta, \phi). \quad (15)$$

Together with the Fourier expansion on $w = M/z$, (14-15) defines a spectral representation in all three coordinates. Fig. (2) shows the results in case of the axisymmetric Boyer-Lindquist initial data, including the computational error behavior in the scalar Ricci tensor. Here, we use the general expansions (8) to probe independently the dependencies on N and L (to go beyond $N = L + 1$ in any truncated series of (14-15)).

Time-evolution of h_{ij} on $z = x + is$ gives rise to burst of radiation which propagates towards quiescent infinity, where the observer's signal is defined on non-negative radii $z \geq 0$. This signal can be calculated by projection according to Cauchy's integral formula,

$$u(r, \theta, \phi, t) = \text{RE} \left\{ \frac{i}{\pi} \int_{-\infty + is}^{\infty + is} \frac{u(z, \theta, \phi, t)}{z - r} dz \right\}, \quad (16)$$

where u denotes a relevant metric component or tensor quantity. Time-evolution on $z = x + is$ is stable when constant translation s , since this preserves reality of the dispersion relation. This can be illustrated by the linear wave-equation for a scalar field $u(t, r)$ in spherical coordinates (t, r, θ, ϕ) with time-symmetric initial data, given by

$$K : \begin{cases} u_{tt}(t, r) = r^{-2} [r^2 u_r(t, r)]_r \\ u(0, r) = u_0(r), \quad u_t(0, r) = 0. \end{cases} \quad (17)$$

By analytic continuation, the equivalent initial value problem K' with complex radial coordinate on $-\infty + is < z < \infty + is$ is

$$K' : \begin{cases} u_{tt}(t, z) = w^4 u_{ww} \quad (w = 1/z) \\ u(0, z) = u_0(z), \quad u_t(0, z) = 0. \end{cases} \quad (18)$$

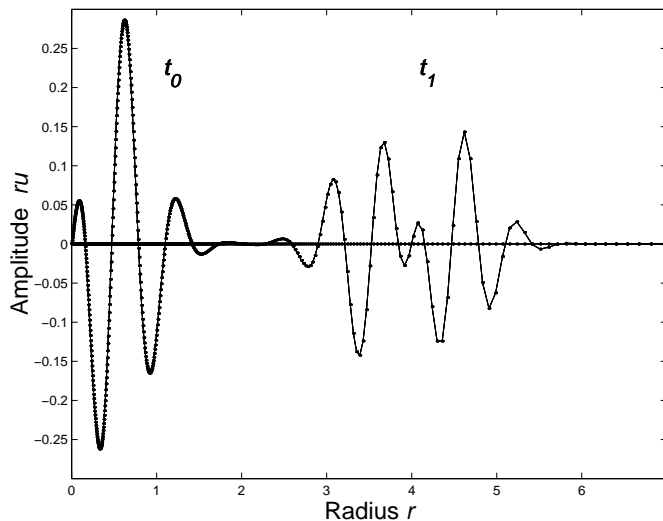


FIG. 3: Signal recovery of a wave propagating to quiescent infinity is shown for a quantity $u(t, z)$ on $z = x + is$, here satisfying the scalar wave equation $u_{tt} = r^{-2}(r^2 u_r)_r$ with time-symmetric initial data at $t = 0$ $u(0, x) = e^{-2x^2} \cos(10x)$ and $u_t(0, x) = 0$. The simulations use the Fourier representation on the complex radius under $w = M/z$ and the wave-equation $u_{tt} = w^4 u_{ww}$ using $N = 1024$ points. Plotted is the quantity ru on $r \geq 0$ for $t_0 = 0$ and $t_1 = 4$. The numerical results (*dots*) accurately track the exact results (*continuous line*, by the method of characteristics). The errors are essentially independent of s , i.e., $4.5e-4$ for $s = 0.5$ and $4.7e-4$ for $s = 1.0$, as implied by analyticity in $s > 0$.

(In general, the analytic continuation of the initial data is the extension of data on (r, θ, ϕ) and $(r, \pi - \theta, \phi + \pi)$). We can implement K' numerically using finite-differencing and leapfrog time-stepping. Fig. (3) shows a representative numerical result, which is verified to satisfy independence of s . The scalar wave-equation with time-symmetric initial data shows the appearance of both left and right movers, the first propagating towards $z = -\infty + is$ and the second propagating towards $z = \infty + is$. Only the right movers are projected onto the observer's non-negative radii $z \geq 0$. The left movers are ultimately dissipated “unseen” in their propagation to $-\infty + is$, while maintaining a contribution to the total mass-energy M in (10).

To conclude, the complex plane offers a unique opportunity for circumventing spacetime singularities and

enabling spectral representations in all three dimensions, consisting of spherical harmonics in the angular coordinates and Fourier series in the complex radial coordinate. This approach creates the most efficient representation of the metric, promising a reduction in computational effort by orders of magnitude compared to standard finite differencing approaches. It will be of interest to take advantage of this approach in time-dependent calculations described by the fully nonlinear equations for general relativity in any of its hyperbolic forms (e.g., [7]).

Acknowledgment. The author thanks the referee for constructive comments. Part of this research is supported by the LIGO Observatories, constructed by Caltech and MIT with funding from NSF under cooperative agreement PHY 9210038. The LIGO Laboratory operates under cooperative agreement PHY-0107417.

[1] Abramovici, A., Althouse, W.E., Drever, R.W.P., et al., 1992, *Science*, 292, 325
 [2] Barish, B., & Weiss, R., 1999, *Phys. Today*, 52, 44
 [3] Acernese, F., et al., 2002, *Class. Quant. Grav.*, 19, 1421
 [4] Bradaschia, C., Del Fabbro, R., di Virgilio, A., et al., 1992, *Phys. Lett. A*, 163, 15

[5] Cook, G.B., 1991, *Phys. Rev. D.*, 44, 2983
 [6] Price, R.H., & Pullin, J., 1994, *Phys. Rev. Lett.*, 72, 3297
 [7] van Putten, M.H.P.M., & Eardley, D.M., 1996, *Phys. Rev. D.*, 53, 3056